JAERI-M
7790

FOCUSING BY BEAMLET STEERING IN TWO-STAGE ACCELERATOR

July 1978

Yoshihiro OHARA

日本原子力研究所
Japan Atomic Energy Research Institute

この報告書は，日本原子力研究所がJAERI-Mレポートとして，不定期に刊行している研究報告書です．入手，複製などのお問合わせは，日本原子力研究所技術情報部（茨城県那珂郡東海村）あて，お申しこしください．

JAERI-M reports, issued irregularly, describe the results of research works carried out in JAERI. Inquiries about the availability of reports and their reproduction should be addressed to Division of Technical Information, Japan Atomic Energy Research Institute, Tokai-mura, Naka-gun, Ibaraki-ken, Japan.

JAERI-M 7790

Focusing by Beamlet Steering in Two-Stage Accelerator

Yoshihiro OHARA

Division of Thermonuclear Fusion Research,

Japan Atomic Energy Research Institute, Ibaraki

(Received July 6, 1978)

Effects of beamlet steering and influence of total beam deflection on the injection efficiency were investigated numerically for the neutral beam injectors of large tokamaks such as JT-60. The beamlet steering by aperture displacement was investigated in the conventional two-stage accelerator by a thin lens approximation. The simultaneous displacement of apertures in the plasma and the gradient grids (or suppressor and the exit grids) turned out to be adequate for beamlet steering. This is due to that the steering characteristics scarcely depend on the field intensity ratio which determines the two-stage ion beam optics, and then the focal point does not change in the wide range of operating conditions of two-stage ion source. Beam focusing in the modified two-stage accelerator was also studied by a thin lens approximation.

Keywords: Two-Stage Acceleration System, Beamlet Steering, Injection Efficiency, Gradient Grid, Beam Optics, Beam Focusing, Field Intensity Ratio, Neutral Beam Injector.

二段加速系におけるビームの集束

日本原子力研究所東海研究所核融合研究部
小 原 祥 裕

（1978年7月6日受理）

ＪＴ－60級の大型トカマク用中性粒子入射装置において,ビームの集束及びビーム軸のずれが入射効率に与える影響について，数値的に評価された。2段加速系における，電極孔の“ずれ”によるビームの集束について，“薄いレンズ”の近似により解析的に調べられた。その結果，プラズマ電極及び傾斜電極の電極孔を同時にずらすことにより，有効にビームの集束ができることがわかった。これは，2段加速系のビーム光学を決定する電界強度比に集束特性がほとんどよらず，イオン源の広い動作領域において，焦点距離が変化しないことを意味している。

Contents

目　　次

1. Introduction

Neutral beam injection heating experiments in the tokamaks such as ORMAK or TFR have demonstrated that the injection of energetic neutral beams is one of the most effective and powerful methods for heating a tokamak plasma. In this method, it is required to extract a beam with low beam divergence to keep high injection efficiency against geometrical losses due to the long beam line and the injection port with limited area between the toroidal coils. This requirement becomes more important as the size of the torus becomes larger. The beam line is composed of neutralizer, pumping region, bending magnet and other required appliances including gate valve or beam dumper, and then the total injector length from the ion source to the injection port of the torus is up to several meters. Consequently, the extraction grid of the ion source is roughly regarded as a point source, when it is viewed from the injection port. In such a case, it is necessary to reduce the beamlet divergence as possible in order to raise the injector efficiency.

On the other hand, larger target plasma thickness demands further increase of beam energy, which induces a rapid decrease of neutralization efficiency above the beam energy around 60 keV. For the ion sources of JT-60 neutral beam injector planned at Japan Atomic Energy Research Institute,[1] the proton beam accelerated at 75 kV is required, where the neutralization efficiency is only 38 %. Then, the total injector efficiency becomes only about 20 - 30 %, due to the geometrical losses and the reionization loss in addition to the small neutralization efficiency.

To improve the injector efficiency at higher beam energy, direct recovery of the energy of unneutralized ions or utilization of negative ions are envisaged, while these methods at high power levels have not been developed yet. In this situation, it is not advisable to ignore the method to steer the indivisual beamlets at the injection port, though the improvement of the injection efficiency may not be large. However, the importance of beamlet steering increases when we design an injector equipped with a few ion sources with large extraction grid rather than many ion sources with small extraction grid. In section 2, the improvement of injection efficiency by the beamlet steering is estimated quantitatively for a typical case of the future injector, where we assume the beam intensity distribution function of each beamlet to be gaussian. For a higher energy ion source, the multiple-stage acceleration system will be

applied to keep high beam power density. In section 3, the beamlet steering by aperture displacement in the two-stage acceleration system is investigated in the thin lens approximation.

2. Effects of Beamlet Steering on Injection Efficiency

We investigated numerically the effects of beamlet steering on the fraction of beam passing through the injection port of the torus. In the numerical model, each beamlet has a axisymmetric guassian beam intensity distribution with e-folding divergence ω.[2] Experimentally, the beam intensity distribution measured calorimetrically is almost gaussian.[3] The center of each beamlet extracted from the aperture at $z = 0$ is directed toward a focal point at $Z = Z_f$. The radius of extraction grid at $Z = 0$ and that of the injection port at $Z = Z_p$ are denoted by R_g and R_p, respectively. The beam intensity I_i at the point (x,y) on the $Z = Z_p$ plane is expressed as follows when i-th beamlet is emitted from a point (X_g^i, Y_g^i) on the extraction grid (See Fig. 1);

$$I_i = \left(\frac{1}{\pi R_o^2}\right) \exp\left\{-\frac{R^2}{R_o^2}\right\} \tag{1}$$

where

$$R_o = Z_p \tan\omega$$

$$R^2 = (X - X_p)^2 + (Y - Y_p)^2$$

$$X_p = \left(\frac{Z_p - Z_f}{Z_f}\right) \cdot X_g^i$$

$$Y_p = \left(\frac{Z_p - Z_f}{Z_f}\right) \cdot Y_g^i$$

Here, the point (X_p, Y_p) is the center of beamlet intensity distribution at $Z = Z_p$. Consequently, the total fraction of the beam which pass through the injection port is obtained by the following equation;

$$F = \frac{1}{n}\iint \sum_{i=1}^{n} I_i \, dS$$

$$= \frac{1}{\pi n R_o^2} \iint \sum_{i=1}^{n} \exp\left\{-\frac{R^2}{R_o^2}\right\} dS \tag{2}$$

where n denotes the number of the beamlets in the extraction grid, and dS is the surface element in the injection port. When Z_f is infinite,

applied to keep high beam power density. In section 3, the beamlet steering by aperture displacement in the two-stage acceleration system is investigated in the thin lens approximation.

2. Effects of Beamlet Steering on Injection Efficiency

We investigated numerically the effects of beamlet steering on the fraction of beam passing through the injection port of the torus. In the numerical model, each beamlet has a axisymmetric guassian beam intensity distribution with e-folding divergence ω.[2] Experimentally, the beam intensity distribution measured calorimetrically is almost gaussian.[3] The center of each beamlet extracted from the aperture at $z = 0$ is directed toward a focal point at $Z = Z_f$. The radius of extraction grid at $Z = 0$ and that of the injection port at $Z = Z_p$ are denoted by R_g and R_p, respectively. The beam intensity I_i at the point (x,y) on the $Z = Z_p$ plane is expressed as follows when i-th beamlet is emitted from a point (X_g^i, Y_g^i) on the extraction grid (See Fig. 1);

$$I_i = \left(\frac{1}{\pi R_o^2}\right) \exp\left\{-\frac{R^2}{R_o^2}\right\} \tag{1}$$

where

$$R_o = Z_p \tan\omega$$
$$R^2 = (X - X_p)^2 + (Y - Y_p)^2$$
$$X_p = \left(\frac{Z_p - Z_f}{Z_f}\right)\cdot X_g^i$$
$$Y_p = \left(\frac{Z_p - Z_f}{Z_f}\right)\cdot Y_g^i$$

Here, the point (X_p, Y_p) is the center of beamlet intensity distribution at $Z = Z_p$. Consequently, the total fraction of the beam which pass through the injection port is obtained by the following equation;

$$F = \frac{1}{n}\iint \sum_{i=1}^{n} I_i \, dS$$
$$= \frac{1}{\pi n R_o^2} \iint \sum_{i=1}^{n} \exp\left\{-\frac{R^2}{R_o^2}\right\} dS \tag{2}$$

where n denotes the number of the beamlets in the extraction grid, and dS is the surface element in the injection port. When Z_f is infinite,

we can obtain the beam fraction to the port without beamlet steering. Using the above equation (2), we calculated the beam fraction through the injection port, where we neglected interception effect by the injector elements such as beam limiter or neutralizer. Parameter survey is performed in the range of Z_p = 5 ∿ 10 m, R_g = 6 ∿ 18 cm and ω = 1.0° ∿ 1.5° at R_p = 20 cm, which will cover typical design values of the injectors for future large tokamaks including JT-60.*)

Figure 2 shows the dependence of the beam fraction passing through the injection port F on the distance between the extraction grid and the injection port Z_p, as a parameter of beamlet divergence. The broken curves indicate the case without beamlet steering, and the solid curves indicate the case with beamlet steering to the center of injection port. Here, the grid radius R_g and the port radius R_p are fixed to 6 cm and 20 cm, respectively. From this figure, we can see that the injection power decreases appreciably with Z_p, when Z_p becomes greater than several meters. However, we can improve the injection power by about several percent by the beamlet steering, when Z_p is below 10 m. This improvement scarcely depends on the beamlet divergence between 1.0° and 1.5°. Figure 3 shows the relation between the beam fraction F and the beamlet divergence ω, when R_g = 6 cm, R_p = 20 cm and $Z_p = Z_f$ = 8 m. This result indicates the importance of reduction of beamlet divergence. We must necessarily obtain the low beamlet divergence below one degree, for the next stage injector. Figure 4 shows the dependence of beam fraction F on Z_p as a parameter of grid radius R_g, where R_p and ω are fixed to 20 cm and 1.0°, respectively. The solid line indicates the case with beamlet steering to the injection port. From this figure, we can see that the improvement in F by the beamlet steering becomes large with the increase of grid radius. The beamlet steering to the port is not necessarily required when $R_g \lesssim 6$ cm. However, it is necessary to focus the beamlet axes to the port, when R_g is greater than 10 cm. From the above numerical estimation for the injectors of large tokamaks such as JT-60, we can see

---

*) In 1977, the design of JT-60 neutral beam injector was modified. The number of the ion sources stacked in each injector unit is reduced from four circular ion sources to two rectangular sources. The initial design values of R_g, R_p and Z_p are 6 cm, 20 cm, and 6.5 m, respectively.[4] In the modified design, the 12×27 cm rectangular extraction grid is adopted, and R_p and Z_p are 22 cm and 8.25 m, respectively.[1] The equivalent radius of the rectangular extraction grid R_g is approximately equal to 10 cm.

that the improvement of injection efficiency by about several % is possible by the beamlet steering. This improvement becomes large with the increase of the size of the extraction grid. In addition, the above results do not include the interception of the beam by the appliances such as gas cell or beam limiter. The beamlet steering becomes important when there exist these intercepting obstacles.

On the other hand, beam deflection by grid misalignment may decrease the injection power appreciably. The grid misalignment about ±0.1 mm is inevitable. Experiment[5] shows that the grid displacement of 0.1 mm makes the beam deflect by about 0.5 degree. Figure 5 shows the influence of beam deflection angle θ on F as a parameter of beamlet divergence ω, where R_g = 6 cm R_p = 20 cm and $Z_p = Z_f$ = 8 m. The radial displacement of the beam center at $Z = Z_p$ is denoted by Δ. This result indicates that the deflection greater than about 0.5 degree is sure to reduce the injection power considerably. Therefore, the accurate beam steering to the center of the injection port is very important for the injector with small acceptance.

3. Beamlet Steering in the Two-Stage Acceleration System

For the ion sources of JT-60 neutral beam injector, a low divergent hydrogen ion beam of several tens of amperes at 75 keV shall be extracted. If the ion source has a configuration of single-stage acceleration, the decrease of beam power flux density is inevitable with the increase of acceleration energies above some level because of the electrical breakdown problem.[6] However, this restriction can be released by decoupling the current extraction stage and the acceleration stage, i.e., by employing a two-stage acceleration system. The two-stage acceleration system is commonly composed of four electrodes (or grids). The first electrode in contact with a source plasma (plasma grid) is held at a positive high potential corresponding to the desired beam energy. The second electrode (gradient grid) is held at an intermediate positive potential to extract an ion beam. The third electrode (suppressor grid) is biased at negative potential to suppress the electron backstreaming from the subsequent beam plasma region. The fourth electrode (exit grid) is grounded electrically. The extraction stage is composed of the plasma grid and the gradient grid and the acceleration stage is composed of the gradient grid, the suppressor grid and the exit grid. As to the two-stage acceleration system, two

that the improvement of injection efficiency by about several % is possible by the beamlet steering. This improvement becomes large with the increase of the size of the extraction grid. In addition, the above results do not include the interception of the beam by the appliances such as gas cell or beam limiter. The beamlet steering becomes important when there exist these intercepting obstacles.

On the other hand, beam deflection by grid misalignment may decrease the injection power appreciably. The grid misalignment about ±0.1 mm is inevitable. Experiment[5] shows that the grid displacement of 0.1 mm makes the beam deflect by about 0.5 degree. Figure 5 shows the influence of beam deflection angle θ on F as a parameter of beamlet divergence ω, where R_g = 6 cm R_p = 20 cm and $Z_p = Z_f$ = 8 m. The radial displacement of the beam center at $Z = Z_p$ is denoted by Δ. This result indicates that the deflection greater than about 0.5 degree is sure to reduce the injection power considerably. Therefore, the accurate beam steering to the center of the injection port is very important for the injector with small acceptance.

3. Beamlet Steering in the Two-Stage Acceleration System

For the ion sources of JT-60 neutral beam injector, a low divergent hydrogen ion beam of several tens of amperes at 75 keV shall be extracted. If the ion source has a configuration of single-stage acceleration, the decrease of beam power flux density is inevitable with the increase of acceleration energies above some level because of the electrical breakdown problem.[6] However, this restriction can be released by decoupling the current extraction stage and the acceleration stage, i.e., by employing a two-stage acceleration system. The two-stage acceleration system is commonly composed of four electrodes (or grids). The first electrode in contact with a source plasma (plasma grid) is held at a positive high potential corresponding to the desired beam energy. The second electrode (gradient grid) is held at an intermediate positive potential to extract an ion beam. The third electrode (suppressor grid) is biased at negative potential to suppress the electron backstreaming from the subsequent beam plasma region. The fourth electrode (exit grid) is grounded electrically. The extraction stage is composed of the plasma grid and the gradient grid and the acceleration stage is composed of the gradient grid, the suppressor grid and the exit grid. As to the two-stage acceleration system, two

models (Model A and Model B) have been considered (See Fig. 6). In the model A, the four grids are all conventional multi-aperture type. In the model B, on the other hand, the first and the second electrodes are multi-aperture type and spherically concave and the third and the fouth electrodes are single disk aperture as is shown in Fig. 6. Here, the feasibility of beamlet steering is examined in the case of two-stage acceleration system, by introducing a thin lens model.

(1) In the first place, we investigated the beamlet steering in the Model A. Two method can be considered for the beamlet steering; one is by aperture displacement, and the other is by curved electrode. In the latter case, extraction grids should be spherically concave so that the curvature center of the grids corresponds to the focal point. For instance, the 24 cm diam. grid shall be concave only by 0.90 mm compared with plain disk grid at the axis, if we need the focal point 8 m apart from the grid.

On the other hand, the focusing by aperture displacement has been investigated both in experiments and in a simple model in thin lens approximation.[5] Here, we applied this simple model to the beamlet steering in the two-stage acceleration system.[7,8] An aperture with a different potential gradient on each side acts as a lens with forcal length $Z_f = 4V/(E_2-E_1)$ for a round aperture and $Z_f = 2V/(E_1-E_2)$ for a slit aperture, respectively. Here, E_1 and E_2 are, respectively, the electric field on each side of the extraction grid, and eV is the energy of the beam which pass through the grid, where e is the ionic charge. The two-stage acceleration system consists of two lenses. The first lens is formed by the electric fields in the first and the second gaps, and the second lens is formed by the electric fields in the second and the third gaps. The electric field in the third gap, however, is almost negligible compared with the others. According to the results of the computer simulation, $E_1 = k_1 v_1/d_1$ with $k_1 = 0.9 \sim 1.0$ and $E_2 = k_2(V_2+V_2)/d_2$ with $k_2 = \sim 1.0$ in the wide range of the beam current density, if the gap distances are enough larger than the aperture radius.[7,9] Here, V_1, V_2+V_3, and V_3 are the potential drop in the first, the second, and the third gaps, respectively. d_1 and d_2 are the distances of the first gap and the second gap, respectively. Therefore, we choose $E_1 = V_1/d_1$ and $E_2 = (V_2+V_2)/d_2$, though in the single-stage acceleration the deflection angle by aperture displacement

agrees well with the experimental results when we put $E_1 = 4V_1/3d_1$ in the plane parallel approximation.[5] The focal length of the first and the second lenses are given as follows; for a round aperture;

$$F_1 = 4V_1/(E_2-E_1) = 4d_2pg(g-p)$$

$$F_2 = 4(V_1+V_2)/(E_3-E_2) = -4d_2(1+p)$$

and for a slit aperture;

$$F_1 = 2V_1/(E_2-E_1) = 2d_2pg(g-p)$$

$$F_2 = 2(V_1+V_2)/(E_3-E_2) = -2d_2(1+p) \ ,$$

where p is the potential ratio defined by $p = V_1/(V_2+V_3)$ and g is the gap ratio defined by $g = d_1/d_2$. There are three cases in the aperture displacement, which are the displacement in the plasma grid(a), the gradient grid(b), and the suppressor grid(c), respectively (See Fig. 7). Case (c) is equivalent to the simultaneous aperture displacement in the plasma and gradient grid. It is natural that the displacement of the exit grid does scarcely cause the deflection of beamlet axes because of the small difference of electric field intensity on the both side of the grid as well as the large beam energy corresponding to the final beam energy. The ratios of reflection angle of the beamlet θ to the radial displacement of the grid Δ are given as follows for each case,

(a) $$\frac{\theta}{\Delta_1} = \left(\frac{1}{F_2} - \frac{1}{d_2-F_1}\right) \cdot \frac{F_1-d_2}{F_1} = \frac{5g-5p-4p^2}{16d_2p(1+p)g}$$

for a round aperture

(b) $$\frac{\theta}{\Delta_2} = \left(\frac{1}{F_2} - \frac{1}{d_2}\right) \cdot \frac{d_2}{F_1} = \frac{(4p+5)(g-p)}{16d_2p(1+p)g}$$

for a round aperture

(c) $$\frac{\theta}{\Delta_3} = \frac{1}{F_2} = \begin{cases} -\dfrac{1}{4d_2(1+p)} & \text{for a round aperture} \\ -\dfrac{1}{2d_2(1+p)} & \text{for a slit aperture.} \end{cases}$$

Figure 8 shows the deflection characteristics for each case as a function

of field intensity ratio f, which is defined by the ratio of electric field intensity in the extraction gap to that in the acceleration gap, and is equal to p/g. According to the results in experiments using a duopigatron ion source with two-stage acceleration system[10] or two-dimensional computer simulation of ion beam trajectories,[7] the field intensity ratio f is an important parameter for the beam optics in the two-stage acceleration system. Namely, the beam optics does scarcely depend on the aspect ratio, gap ratio g, and potential ratio p, so long as f is fixed. The smaller beam divergence can be obtained as the ratio f becomes smaller. However, higher preveance can be obtained with the increase of f. To obtain high perveance and low divergent beam, the value of f around 0.5 is adequate. From the results in Fig. 8, the first two cases are inadequate in that the displacement characteristic depends largely on the parameter f. In the third case, however, the deflection does scarcely depend on f, in comparison with the other cases. The good displacement must be larger than the mechanical inaccuracy $\pm\sim 0.1$ mm, but far smaller than the aperture diameter to keep good beam optics;

$$\text{Mechanical inaccuracy } \pm\ 0.1 \text{ mm} \ll \Delta \ll \text{Aperture Diameter.}$$

Now, when f = 0.5, $d_1 = d_2 = 6$ mm, focal length $Z_f = 8$ m, and the radius of the extraction grid is 12 cm, the displacement Δ_3 at the periphery of the grid is about 0.5 mm for a round aperture. This is the practical value of the displacement. Consequently, the beamlet steering by aperture displacement is possible for the case of two-stage configuration.

(2) In the second place, we applied the thin lens theory to the analysis of beam steering in the Model B extraction system. The optimum configuration of this system is investigated in some detail by the computer simulation presented in Ref. (11) and (12). In this system, the third grid is biased at relatively high negative voltage above several tens of kilovolts, because of the larger aperture diameter compared with that in the Model A. With the variation of beam current, the biased voltage will be changed so that the electron backstreaming should not be caused. We can expect that the forth electrode plays an important role in the lens action as well as the third electrode. The focal lengths of the lens in the third and the fourth electrode are given as follows, respectively;

$$F_1 = -\frac{4d_2d_3(V_1+V_2+V_3)}{d_2V_3+d_3(V_2+V_3)}$$
$$F_2 = \frac{4d_3(V_1+V_2)}{V_3} \tag{7}$$

Here, we examined the three cases in the aperture displacement, that is, the displacement of the third electrode(a), the fourth electrode(b), and the simultaneous displacement of the third and the fourth electrode(c) (See Fig. 9). The ratios of reflection angle of the beam θ to the radial displacement of the electrode Δ are given as follows for each case.

$$\text{(a)}\quad \frac{\theta}{\Delta_1} = -\frac{1}{F_1}+\frac{d_3}{F_1F_2}$$
$$\text{(b)}\quad \frac{\theta}{\Delta_2} = \frac{1}{F_2} \tag{8}$$
$$\text{(c)}\quad \frac{\theta}{\Delta_3} = \frac{1}{F_1}+\frac{1}{F_2}-\frac{d_3}{F_1F_2}$$

Table I shows the dependence of θ/Δ on the voltage $(-V_3)$ biased in the third electrode, where d_1 = 5 cm, d_2 = 2 cm, V_1 = 25 kV and V_2 = 50 kV. Table II shows the dependence of θ/Δ on the acceleration voltage V_2 applied to the second electrode, where d_1 = 5 cm, d_2 = 2 cm, V_1 = 25 kV, and V_2 = 25 kV. From this results, we can see that the case (a) is more advantageous than the others in that θ/Δ dose scarcely depend on V_2 or V_3, which are closely related to the total beam energy, beam optics and the extraction current.

The analysis here by the thin lens approximation has some limitations, because the above results include no dependence on the radius of the apertures or the thickness of the electrodes. In general, the error in the above analysis increases appreciably when the radius of the apertures becomes comparable or smaller than the thickness of the electrode or becomes larger than the gap distances between the electrodes. In the Model A, however, the error may be small because we use the electric field intensity E_1, E_2 and E_3 obtained in the two-dimensional computer simulation.

4. Conclusion

The beam line length of the injector becomes up to several to ten meters with the increase of target plasma thickness. The long beam line

$$F_1 = -\frac{4d_2d_3(V_1+V_2+V_3)}{d_2V_3+d_3(V_2+V_3)}$$
$$F_2 = \frac{4d_3(V_1+V_2)}{V_3} \tag{7}$$

Here, we examined the three cases in the aperture displacement, that is, the displacement of the third electrode(a), the fourth electrode(b), and the simultaneous displacement of the third and the fourth electrode(c) (See Fig. 9). The ratios of reflection angle of the beam θ to the radial displacement of the electrode Δ are given as follows for each case.

$$\text{(a)}\quad \frac{\theta}{\Delta_1} = -\frac{1}{F_1}+\frac{d_3}{F_1F_2}$$
$$\text{(b)}\quad \frac{\theta}{\Delta_2} = \frac{1}{F_2} \tag{8}$$
$$\text{(c)}\quad \frac{\theta}{\Delta_3} = \frac{1}{F_1}+\frac{1}{F_2}-\frac{d_3}{F_1F_2}$$

Table I shows the dependence of θ/Δ on the voltage $(-V_3)$ biased in the third electrode, where d_1 = 5 cm, d_2 = 2 cm, V_1 = 25 kV and V_2 = 50 kV. Table II shows the dependence of θ/Δ on the acceleration voltage V_2 applied to the second electrode, where d_1 = 5 cm, d_2 = 2 cm, V_1 = 25 kV, and V_2 = 25 kV. From this results, we can see that the case (a) is more advantageous than the others in that θ/Δ dose scarcely depend on V_2 or V_3, which are closely related to the total beam energy, beam optics and the extraction current.

The analysis here by the thin lens approximation has some limitations, because the above results include no dependence on the radius of the apertures or the thickness of the electrodes. In general, the error in the above analysis increases appreciably when the radius of the apertures becomes comparable or smaller than the thickness of the electrode or becomes larger than the gap distances between the electrodes. In the Model A, however, the error may be small because we use the electric field intensity E_1, E_2 and E_3 obtained in the two-dimensional computer simulation.

4. Conclusion

The beam line length of the injector becomes up to several to ten meters with the increase of target plasma thickness. The long beam line

diminishes the effectiveness of beamlet steering, and imposes the further improvement of beamlet optics. In the initial design of JT-60 injector where 4 ion sources with 12 cm diam. extraction grid are applied, the improvement of injection power by beamlet steering is only several percent. Now, we expect the improvement above 10 %, in the present design where 2 ion sources with larger extraction grid (12 × 27 cm rectangular grid) are used.

The accurate orientation of the total beam to the center of the injection port is very important for the injector with small acceptance. The beam deflection above 0.5 degree is sure to decrease the injection efficiency appreciably.

On the other hand, the beamlet steering by aperture displacement was investigated in the two-stage acceleration system by introducing a thin lens approximation. It is found that the simultaneous aperture displacement in the plasma and gradient grids (or suppressor and exit grids) is adequate in that the steering characteristic does scarcely depend on the field intensity ratio which determines the two-stage ion beam optics.

Acknowledgement

The author would like to express his appreciation to Dr. S. Matsuda for his valuable discussions. Thanks are also due to Drs. H. Shirakata, Y. Obata and S. Mori for their support and encouragement.

diminishes the effectiveness of beamlet steering, and imposes the further improvement of beamlet optics. In the initial design of JT-60 injector where 4 ion sources with 12 cm diam. extraction grid are applied, the improvement of injection power by beamlet steering is only several percent. Now, we expect the improvement above 10 %, in the present design where 2 ion sources with larger extraction grid (12 × 27 cm rectangular grid) are used.

The accurate orientation of the total beam to the center of the injection port is very important for the injector with small acceptance. The beam deflection above 0.5 degree is sure to decrease the injection efficiency appreciably.

On the other hand, the beamlet steering by aperture displacement was investigated in the two-stage acceleration system by introducing a thin lens approximation. It is found that the simultaneous aperture displacement in the plasma and gradient grids (or suppressor and exit grids) is adequate in that the steering characteristic does scarcely depend on the field intensity ratio which determines the two-stage ion beam optics.

Acknowledgement

The author would like to express his appreciation to Dr. S. Matsuda for his valuable discussions. Thanks are also due to Drs. H. Shirakata, Y. Obata and S. Mori for their support and encouragement.

References

1) S. Matsuda, Y. Arakawa, H. Horiike, T. Itoh, U. Kondoh, Y. Ohara, T. Ohga, Y. Okumura, T. Shibata, H. Shirakata and S. Tanaka: Japan Atomic Energy Research Institute. Report, JAERI-M 7655 (1978) [in Japanese].
2) S. Matsuda: Japan, J. Appl. Phys. 13, (1974) 1630.
3) Y. Ohara, S. Matsuda, H. Shirakata and S. Tanaka: Japan Atomic Energy Research Institute Report, JAERI-M 6438 (1976), (in Japanese).
4) S. Matsuda, M. Akiba, Y. Arakawa, H. Horiike, T. Itoh, U. Kondoh, Y. Ohara, T. Ohga, T. Shibata, H. Shirakata, T. Sugawara, and S. Tanaka: Proc. of the 2nd Large Tokamak Meeting, Princeton, 1976 (IAEA, Vienna, 1976).
5) L.D. Stewart, J. Kim and S. Matsuda: Rev. Sci. Instrum. 46, (1975) 1193.
6) E. Thompson: Proc. 2nd Sympo. on Ion Sources and Formation of Ion Beams, California, 1974 (Lawrence Berkeley Lab., Berkeley, 1975) Paper II-7.
7) Y. Ohara: Japan Atomic Energy Research Institute Report, JAERI-M 6813 (1976).
8) J.H. Whealton: Rev. Sci. Instrum. 48, (1977) 1428.
9) J. Kim, J.H. Whealton and G. Schilling: J. Appl. Phys. 49, (1978) 517.
10) Y. Ohara, Y. Arakawa, H. Horiike, U. Kondoh, S. Matsuda, T. Ohga, Y. Okumura and H. Shirakata: Proc. 7th Symp. on Engineering Problems of Fusion Research, Knoxville (1977) 273.
11) T. Sugawara and Y. Ohara: Japan J. Appl. Phys. 14, (1975) 1029.
12) Y. Ohara and T. Sugawara: Japan Atomic Energy Research Institute Report, JAERI-M 5929 (1974).

Table I Deflection characteristics vs V_3, where d_1=50 mm, d_2=20mm, V_1=25 kV, and V_2=50 kV

V_3 (kV)	θ/Δ_1 (deg/mm)	θ/Δ_2(deg/mm)	θ/Δ_3(deg/mm)
-10	+0.277	+0.095	-0.181
-20	+0.338	+0.191	-0.147
-30	+0.381	+0.286	-0.094
-40	+0.410	+0.382	-0.028

Table II Deflection characteristic vs. V_2, where d_1=50 mm, d_2=20 mm, V_1=25 kV, and V_3=-25 kV

V_2 (kV)	θ/Δ_1 (deg/mm)	θ/Δ_2 (deg/mm)	θ/Δ_3 (deg/mm)
25	+0.376	+0.358	-0.018
50	+0.361	+0.239	-0.122
75	+0.349	+0.179	-0.170

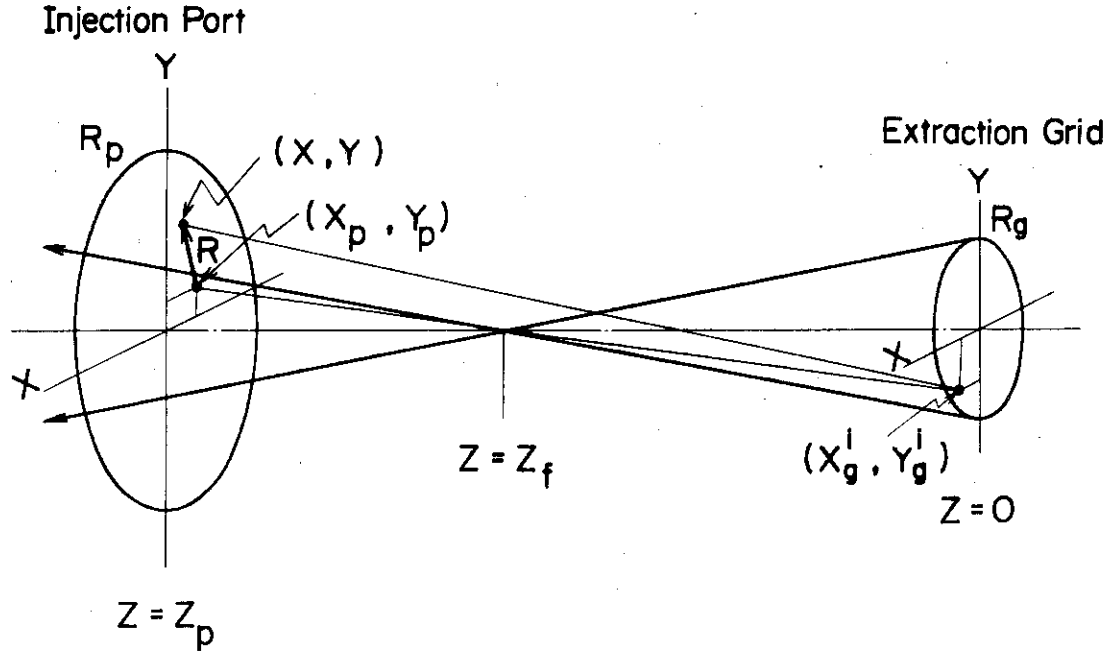

Fig. 1 Schematic illustration of the extraction grid and the injection port. The point (X_p, Y_p, Z_p) indicates the center of beamlet emitted from the point (X_g, Y_g, 0).

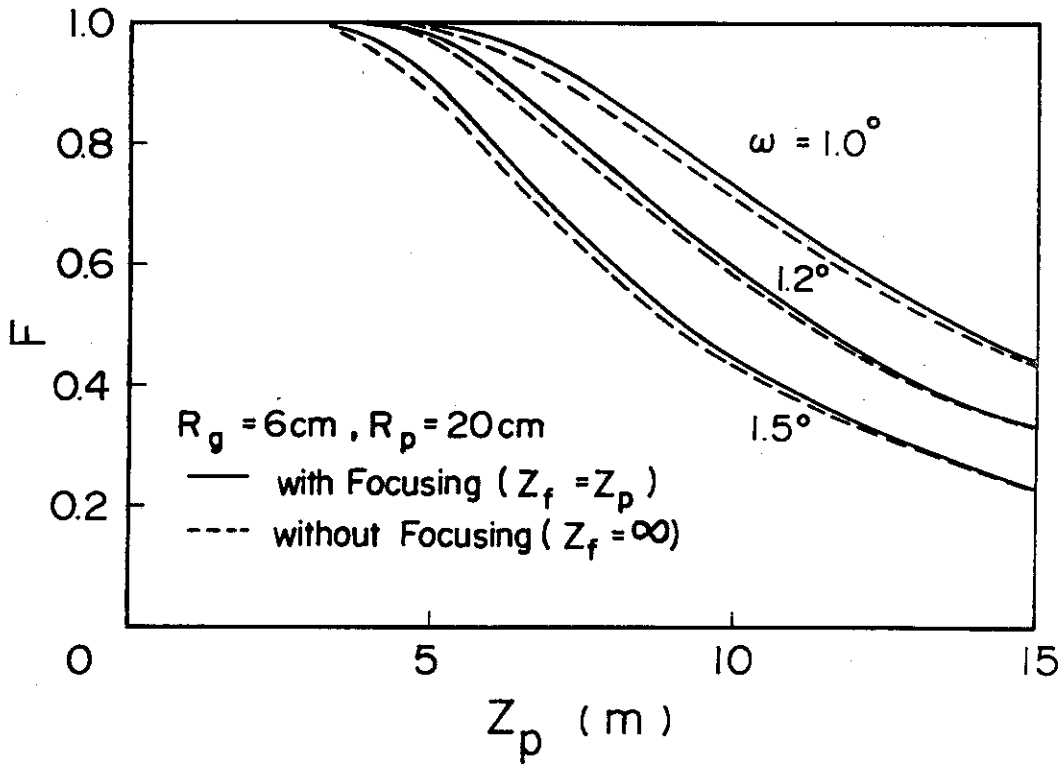

Fig. 2 Dependence of the beam fraction passing through the injection port F on the beam line length Z_p, as a parameter of beamlet divergence. The broken curves indicate the case without beamlet steering.

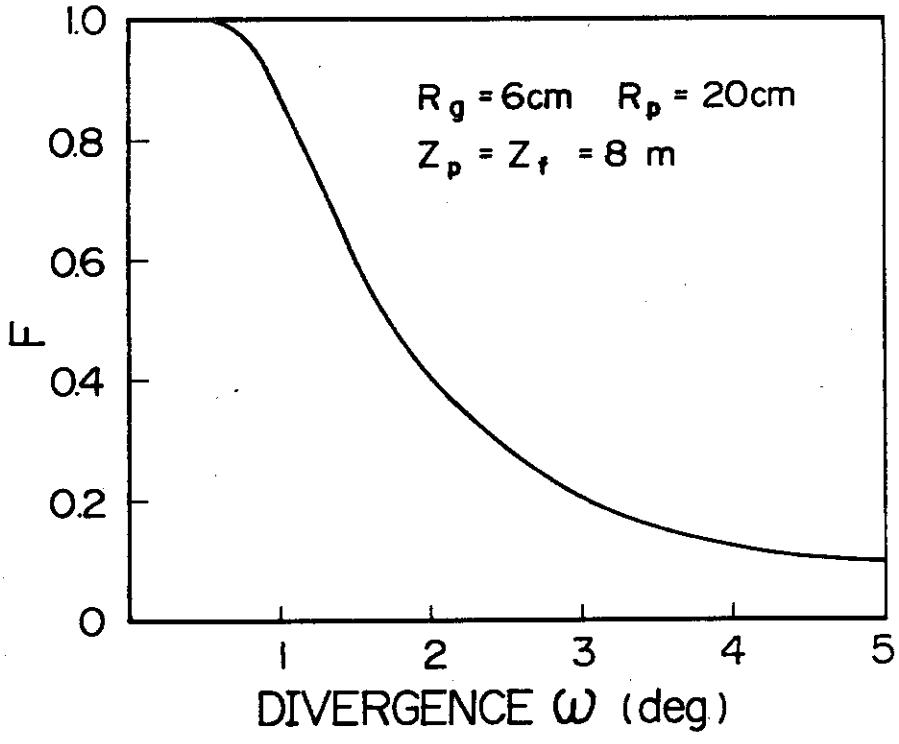

Fig. 3 Relation between the beam fraction F and the beamlet divergence ω, when R_g=6 cm, R_p=20 cm and Z_p=Z_f=8 m.

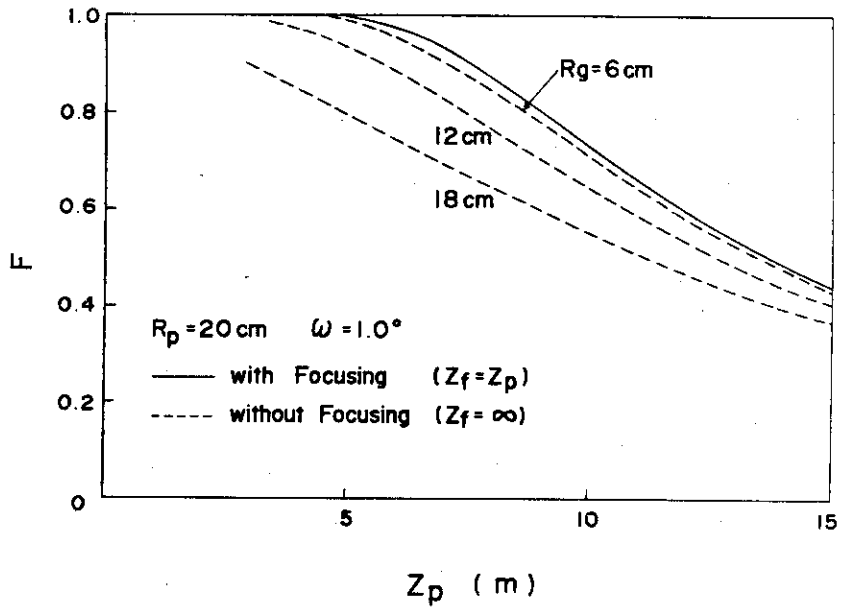

Fig. 4 Dependence of the beam fraction F on the beamline length Z_p, as a parameter of grid radius R_g, where R_p and ω are fixed to 20 cm and 1.0°, respectively. The solid line indicates the case with beamlet steering.

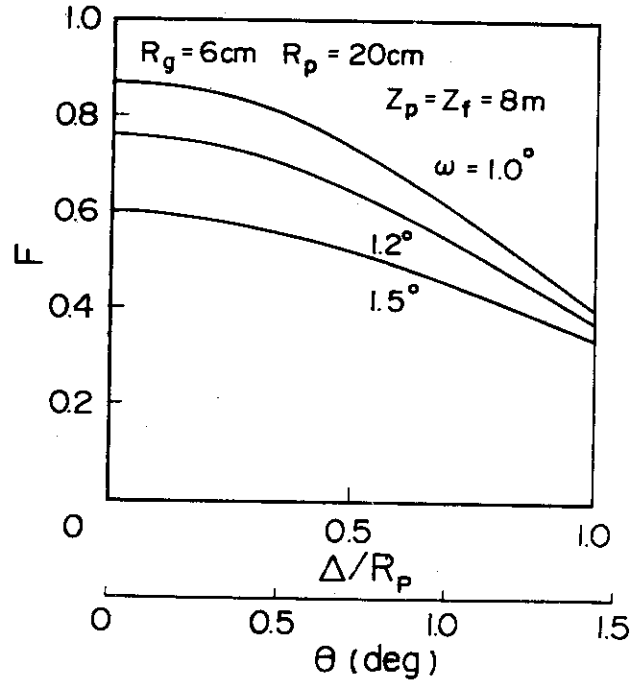

Fig. 5 Relation between the beam deflection angle θ and the beam fraction F, as a parameter of beamlet divergence ω. The radial displacement of the beam at $Z=Z_p$ is denoted by Δ.

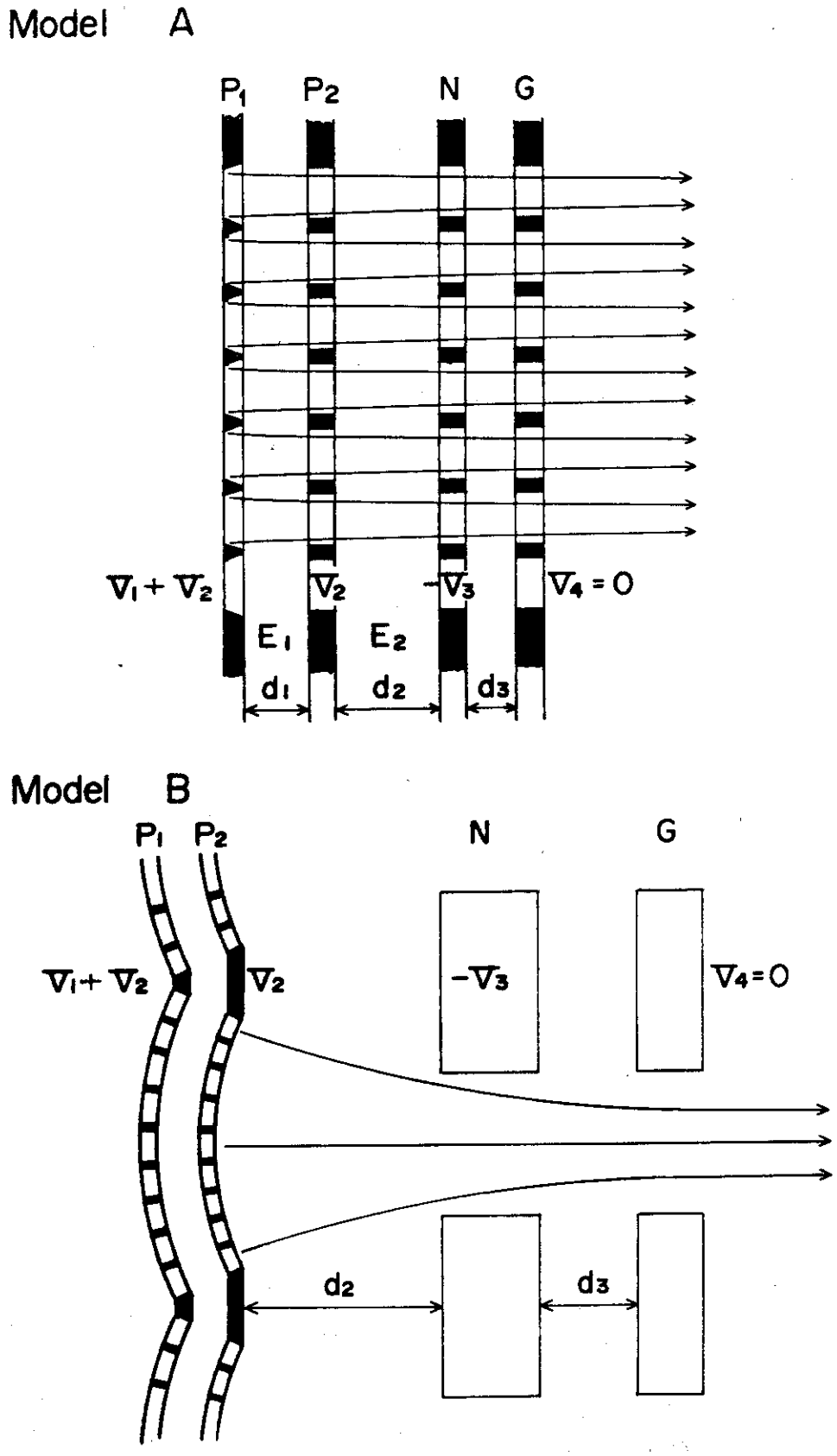

Fig. 6 Two models of the two-stage acceleration system (Model A and Model B).

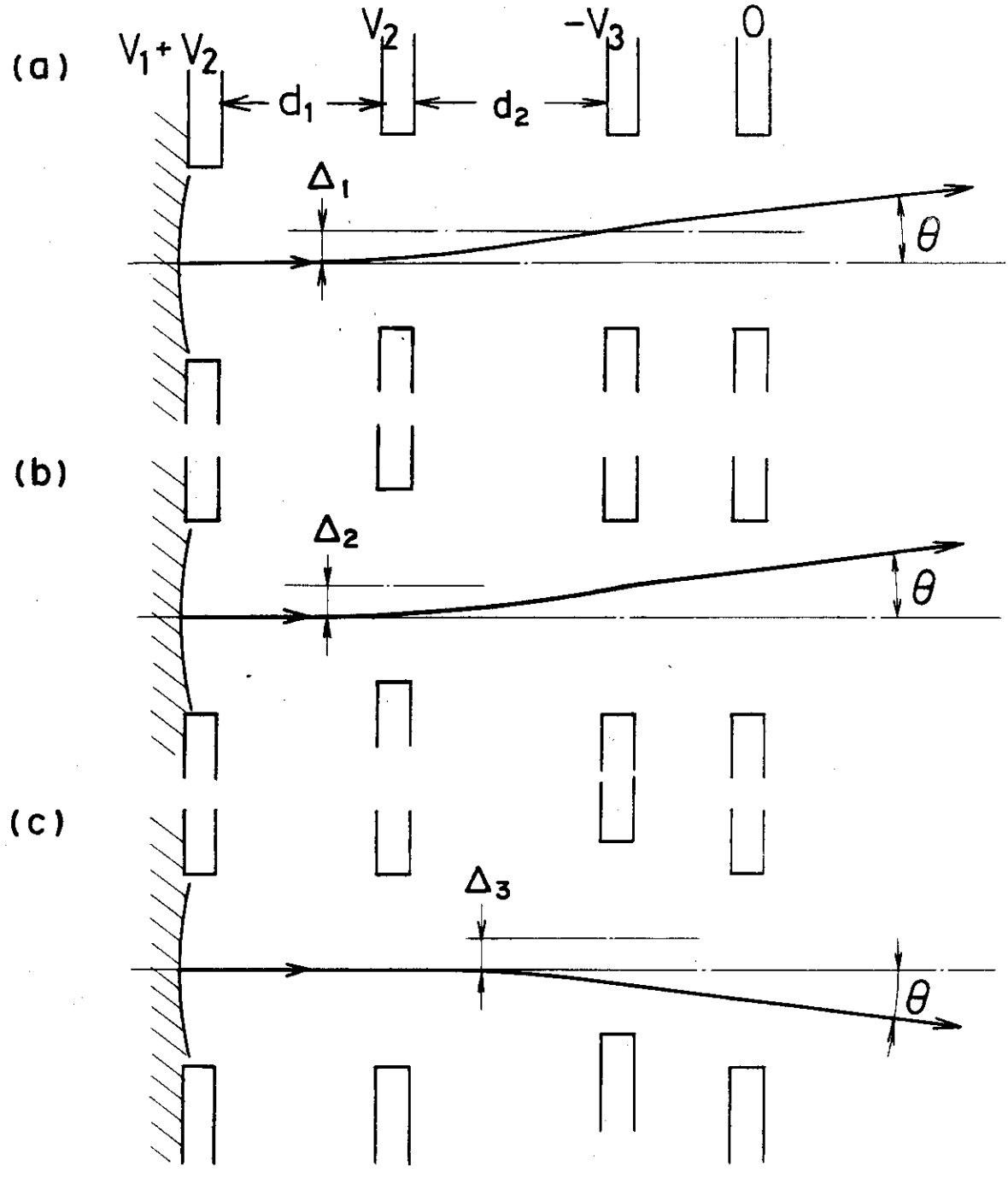

Fig. 7 Three cases of aperture displacement in the Model A, which are the displacements in the plasma grid (a), the gradient grid (b), and the suppressor grid (c), respectively.

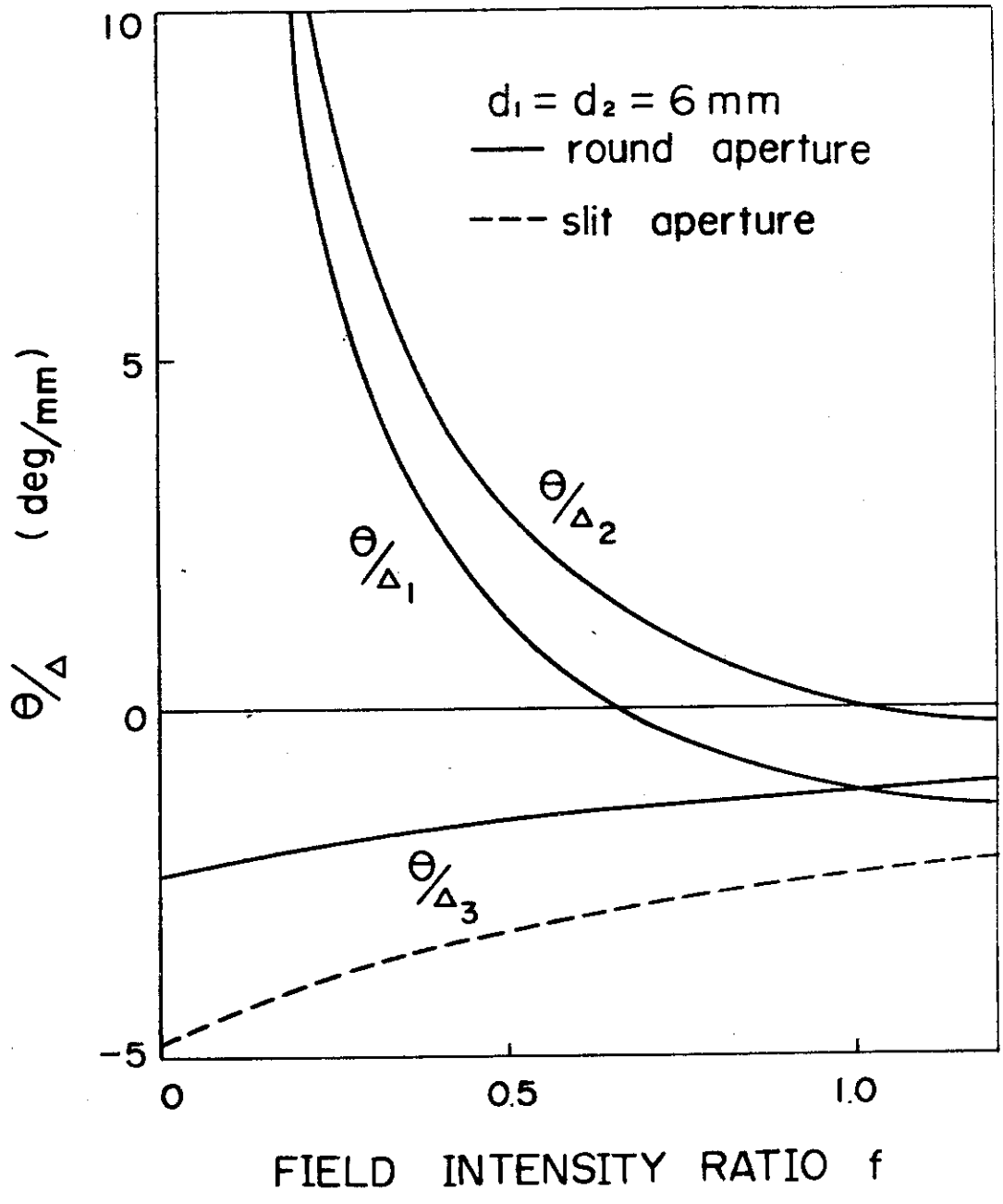

Fig. 8 Deflection angle divided by the aperture displacement θ/Δ for each case in the Model A system as a function of field intensity ratio f.

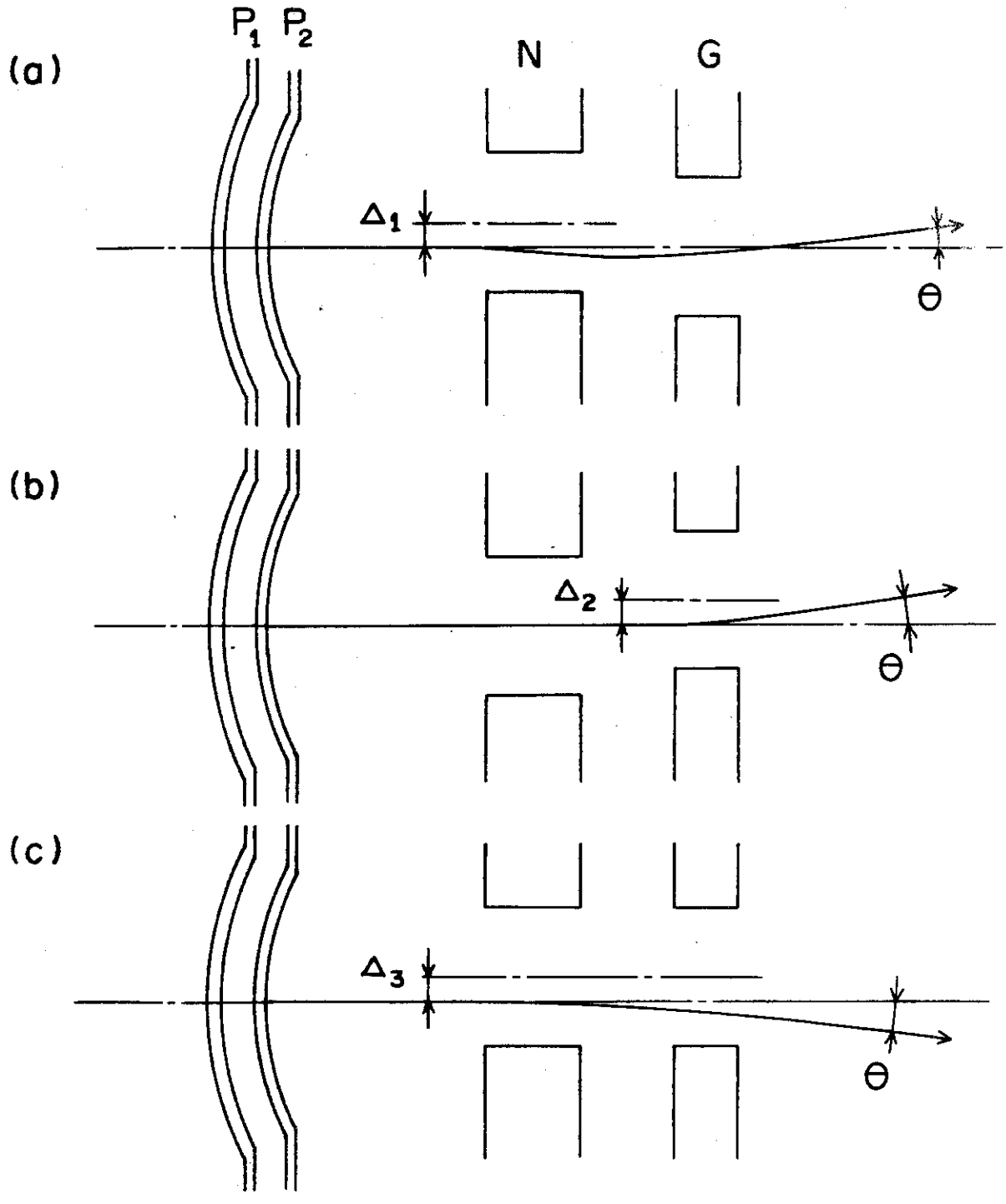

Fig. 9 Three cases of the aperture displacement in the Model B, which are the displacements of the suppressor grid (a), the exit grid (b) and the simultaneous displacement of the suppressor and the exit grids (c).